Supplementary Information

1. Data

Since 1994, a large-scale ground inventory has been conducted on numerous permanent sample plots established on the forested areas across the boreal region of Alaska. Inventory crew collected size (DBH and percentage cover) and status of all the plant species including tree, shrub, herbaceous vascular, and non-vascular species on an annual basis (1). The Alaska boreal forest, the largest forest component of the Alaska landscape, is characteristic of some of the most severe climatic conditions in the world with short growing seasons. Soil parent materials vary greatly from alluvial, loess, glacial, and lacustrine deposits to various bedrock types, with discontinuous permafrost present throughout the region. The sample area, stretching over 300,000 km^2 from Fairbanks, AK in the north to the Kenai Peninsula in the south and the International Boundary in the east (**Fig. S1**), represents a wide range of species composition and physiographic conditions. A set of permanent sample plots were used to capture the dynamics of 283 coexisting plant species in the region (**Table S1**).

The fixed-size permanent sample plots, each square in shape and 0.04 ha in size, were re-measured with a 5-year interval. The attributes measured include diameter at breast height, height, tree status, the percentage cover of non-tree species, elevation, percentage slope, thickness of organic horizons, and number of snags. The number of *Picea glauca* individuals in comparative relationship to the total number of trees on a plot was calculated to represent the sampling effect, as *Picea glauca* has the highest individual ANPP among all the tree species that almost doubles the second highest species (*Betula neoalaskana*) (**Fig. S2**). In addition, two time indicators (T_1, T_2) were introduced to represent from which inventory a particular observation was made. From the 603 established permanent sample plots, 440 were selected for this study because they have been measured at least twice and have not experienced any crown fire or logging between two consecutive inventories.

For individual trees, we calculated the above-ground net primary productivity (ANPP) using the following equation:

$$ANPP_{ijk} = (V_{2,ijk} - V_{1,ijk}) / (y_2 - y_1), \qquad \text{(M.1)}$$

where the ANPP of the *k*th tree in species *i* on plot *j* is average annual increment in above-ground biomass (AGB) of that tree from year y_1 to y_2. V_1 and V_2 represent AGB of that tree at year y_1 and y_2, respectively, calculated from its measured DBH using the species-specific biomass equations developed for the Alaska boreal forest(2). *ANPP* is zero for a tree that died between year y_1 and y_2. ANPP is the part of NPP that occurs aboveground and is composed of wood and foliage productivity, whereas root growth represents belowground productivity, which is extremely difficult to measure and contributes to ecosystem services, such as carbon storage, but not to harvested fiber. ANPP of trees was selected as the response variable of our spatio-temporal model, as it is more routinely measured and represents wood production, a surrogate for economically important fiber production.

The total tree ANPP of a community (*TNPP*) was then calculated using the following equation:

$$TNPP_j = \left(\sum_i \sum_k V_{2,j} - \sum_i \sum_k V_{1,j} + \sum_i \sum_k IG_j + \sum_i \sum_k MT_j \right) \Big/ (y_2 - y_1), \tag{M.2}$$

where $\Sigma\Sigma V_{2,j}$ *and* $\Sigma\Sigma V_{1,j}$ represent total AGB of trees on plot *j* that were alive at year y_2 and y_1, and $\Sigma\Sigma IG_j$ and $\Sigma\Sigma MT_j$ are respectively total AGB of ingrowth and mortality on plot *j* between year y_1 and y_2.

The AGB of shrub, herbaceous vascular, and non-vascular species was calculated based on the observed percentage cover and average height of that species using the species-specific biomass equations calibrated for interior Alaska(3). On average, tree species accounts for most of the total AGB, whereas shrub, herbaceous vascular, and non-vascular species accounts for less than 10 percent of the total AGB (**Fig. S3**).

In our empirical analysis, the authors relied upon two *measures of biodiversity*, which are widely used in both ecological and economic research:

– Shannon index, *H*, which measures biodiversity with an entropic approach:

$$H_j = -\sum_{i=1}^{n} \frac{V_{ij}}{V_j} \ln\left(\frac{V_{ij}}{V_j} \right), \tag{M.3}$$

where V_{ij} presents the live aboveground biomass of species *i* on plot *j*, and V_j the total live aboveground biomass of Plot *j*.

– Simpson index, *D*. The same index known as the Herfindahl-Hirschman index (HHI) is a measure of diversity widely used in competition law, antitrust, and management:

$$D_j = 1 - \sum_{i=1}^{n} \left(\frac{V_{ij}}{V_j} \right)^2 . \tag{M.4}$$

2. The Spatio-Temporal Model

In investigating the empirical relationship between biodiversity and ANPP, the authors elected to develop a regression-based spatio-temporal model to account for spatial autocorrelation which has been found prevalent in attributes of the Alaska boreal forest, such as stand basal area, tree diversity, and forest productivity (4). Failing to account for such correlation in space will render model outputs less reliable (5). Although an alternate statistical approach, namely structural equation modeling (SEM), has been employed in ecology for the testing of causal relationship in complex datasets, spatial autocorrelation violates basic SEM assumptions and remains difficult to model in a SEM framework (6). Furthermore, computational constraints of existing SEM software have limited applicability of SEM on this study because our dataset consisted of tree records from 40,526 spatially explicit locations.

Autocorrelation in both space and time were accounted for in our model to avoid biased or inconsistent coefficient estimates and significance levels. Spatial autocorrelation in above-ground net primary productivity was estimated using a nonparametric spatial covariance function. This method incorporates a smoothing spline to measure the correlation between values (in our case ANPP) from pairs of samples over a continuous function of the distance separating samples, without assuming any functional form *a priori*. However, because of the large size (over 40,000 entries) of our spatially explicit dataset, it was not feasible to estimate spatial autocorrelation based upon the entire dataset due to computational constraints. To this end, a bootstrap approach(7) was used to quantify the spatial covariance function. We iteratively and randomly selected approximately 10% of the data, and then repeated this procedure 500 times. From this distribution of 500 replicated estimates of the spatial covariance function, the mean was determined and 95% confidence intervals were estimated as the 0.025% and 0.975% quantiles of the distribution(7).

Across the 500 replications, the mean number of sampling locations selected (from the 40,526 locations) per iteration was 4056, and ranged from 3838 to 4216. The authors detected spatial correlation in ANPP (**Fig. S4**), and estimated a mean local spatial autocorrelation (the correlation as the spatial distance between pairs of sample ANPP values approaches 0) of 0.09 and a range of spatial dependence (the lag distance at which spatial autocorrelation approaches 0) of ~10 km. Moreover, the functional form of the spatial covariance function over lag distance suggested that the use of spherical model would be the most appropriate one to use as an error term when assessing the significance of potential explanatory variables on ANPP.

To avoid compromised type-I error rates and severe artifacts associated with common model selection procedures, hierarchical partitioning (HP) was used here to evaluate the goodness-of-fit of all the possible combinations of explanatory variables in determining the average independent contribution of each variable(8). The threshold value of independent contribution was set at 8 percent, the average value with 12 explanatory variables (**Table S2**). Diversity variables and time indicators were always present in the model, regardless of their independent contribution. HP was conducted with the hier.part package of the R program. Total aboveground biomass, V, the number of snags, S, and the frequency of *Picea glauca*, P, were selected as control variables as each of them has an independent contribution to the individual ANPP no less than 8 percent (**Fig. S5**). Biodiversity $\omega(\mathbf{s})$ was represented in this model by the full quadratic forms of Shannon index, H, and Simpson index, D, both of which provide a continuous measure of biodiversity.

The following spatio-temporal model was developed to examine the effect of biodiversity on individual plant productivity (ANPP model):

$$ANPP_{ijk}(\mathbf{s}, \omega) = \alpha_0 + \alpha_1 \cdot \omega(\mathbf{s}) + \alpha_2 \cdot T_1(\mathbf{s}) + \alpha_3 \cdot T_2(\mathbf{s}) + \boldsymbol{\beta} \cdot \mathbf{z}(\mathbf{s}) + \varepsilon_i(\mathbf{s}), \qquad \text{(M.5)}$$

where $\mathbf{s} = (\lambda, \varphi)' \in \mathfrak{D} \subset IR^2$ represents the geographic location of a plot *j* within the Alaska boreal region $\mathfrak{D}$. In this specification, individual ANPP at geographic location **s** is a linear function of the biodiversity of the same plot, the temporal indicators T_1 and T_2, and the vector of control variables **z**. $\varepsilon_i(\mathbf{s})$ is a spatially autocorrelated residual term best described as a spherical variogram 2ς model with intrinsic stationarity and isotropic covariance. α_0, α_1, α_2, α_3, $\boldsymbol{\beta}$, and ς are parameters to be estimated with generalized least squares (GLS). The two time indicators (T_1, T_2) were introduced to the model to account for potential factors of ANPP that are not controlled for by the explanatory variables in this model, such as the temporal difference in sample plot locations.

Due to computational constraints, a bootstrap approach was used to obtain model coefficients and predicts. The authors iteratively and randomly selected approximately 1% of the data from the entire dataset, obtained GLS estimates, log-likelihood, and predictions across the full observed range of each biodiversity measure for the sensitivity analysis, and then repeated this procedure 1,000 times. From the distribution of 1,000 replicated estimates and predicts of the model, the mean and 95% confidence intervals were determined.

Estimates and goodness-of-fit of the spatio-temporal model are summarized in **Table S3**. All the coefficients are significant at the 5 percent level. The signs of total aboveground biomass, *V*, and the frequency of *Picea glauca*, *P*, are consistently positive, indicating an expected positive effect of total biomass and sampling effect on individual tree ANPP. The negative signs of the number of snags, *S*, and the two temporal indicators T_1 and T_2 are also consistent. The two goodness-of-fit measures Akaike information criterion (AIC) and Bayesian information criterion (BIC) were calculated based on the average log-likelihood values of all the bootstrap iterations, the number of coefficients, and the total number of observations. The present spatio-temporal models were able to capture an interaction in space and time, as the negative coefficients of T_1 and T_2 indicate a declining trend of ANPP over time, which is likely caused by the fact that most plots in the third and fourth inventories are centered around Fairbanks, AK, where the sites are in general less productive.

SI REFERNCES

1. Malone T, Liang J, & Packee. EC (2009) Cooperative Alaska Forest Inventory. (Gen. Tech. Rep. PNW-GTR-785, USDA Forest Service, Pacific Northwest Research Station, Portland, OR), p 42.
2. Yarie J, Kane ES, & Mack MC (2007) Aboveground biomass equations for trees of Interior Alaska. (Agricultural and Forestry Experiment Station, University of Alaska Fairbanks, Fairbanks, AK), p 15.
3. Mack M*, et al.* (2008) Recovery of Aboveground Plant Biomass and Productivity After Fire in Mesic and Dry Black Spruce Forests of Interior Alaska. *Ecosystems* 11(2):209-225.

4. Liang J (2012) Mapping large-scale forest dynamics: a geospatial approach. *Landscape Ecol.* 27(8):1091-1108.
5. Legendre P (1993) Spatial autocorrelation: trouble or new paradigm? *Ecology* 74(6):1659-1673.
6. Lamb EG, Mengersen KL, Stewart KJ, Attanayake U, & Siciliano SD (2014) Spatially explicit structural equation modeling. *Ecology* 95(9):2434-2442.
7. Efron B & Tibshirani RJ (1993) *An Introduction to the Bootstrap* (Chapman & Hall, New York) p 436.
8. Chevan A & Sutherland M (1991) Hierarchical partitioning. *Amer. Statistician* 45:90-96.

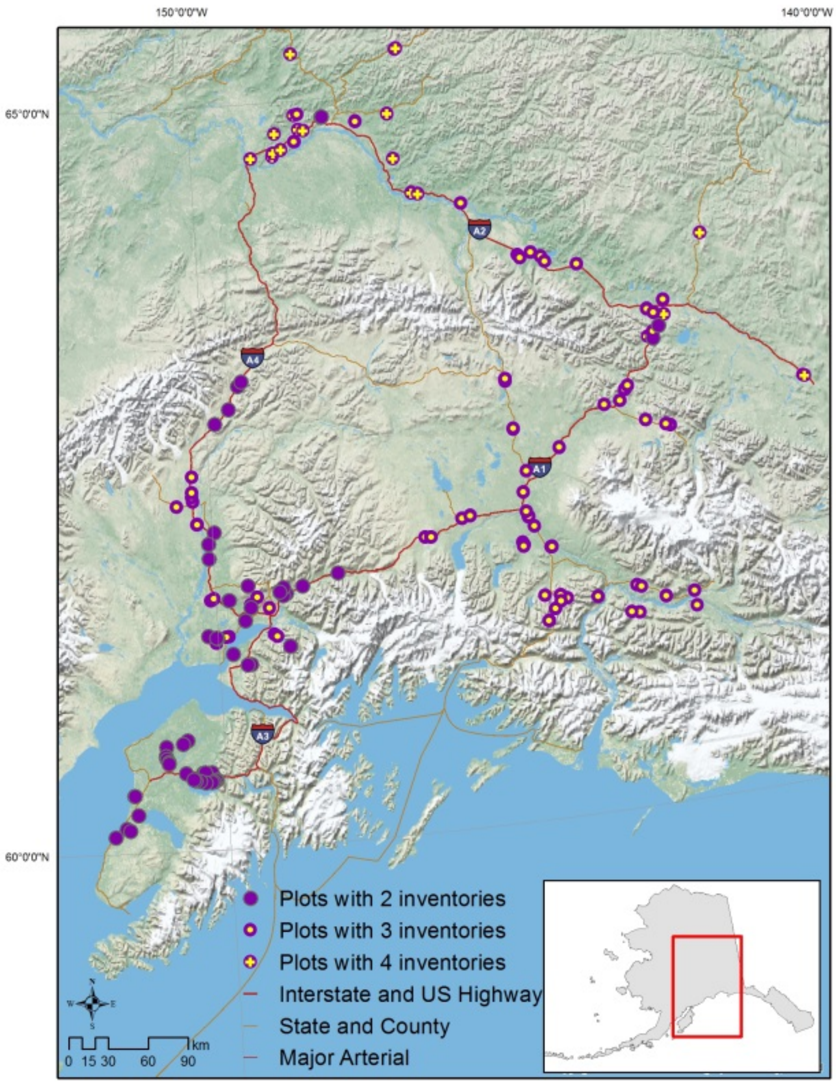

Fig. S1 Geographic distribution of the 440 permanent sample plots and their relative location within the State of Alaska (inset). All the plots have been measured at least twice with an interval of 5 years, 280 have been measured in 3 inventories, and 65 in 4 inventories, making a total of 785 plot observations.

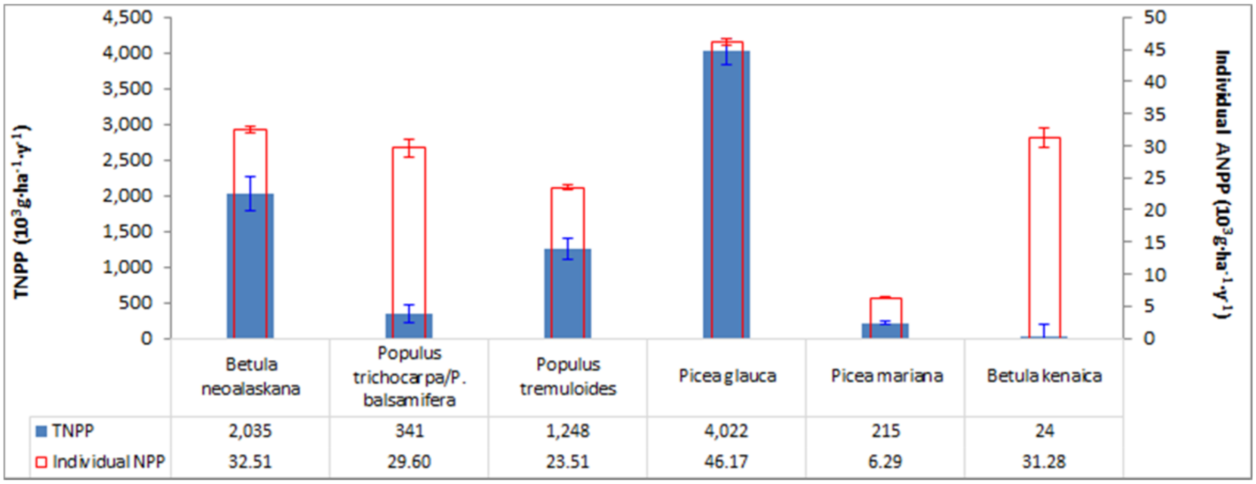

Fig. S2 Total net primary productivity (TNPP) (primary axis) and average individual ANPP (secondary axis) by tree species with standard error bars.

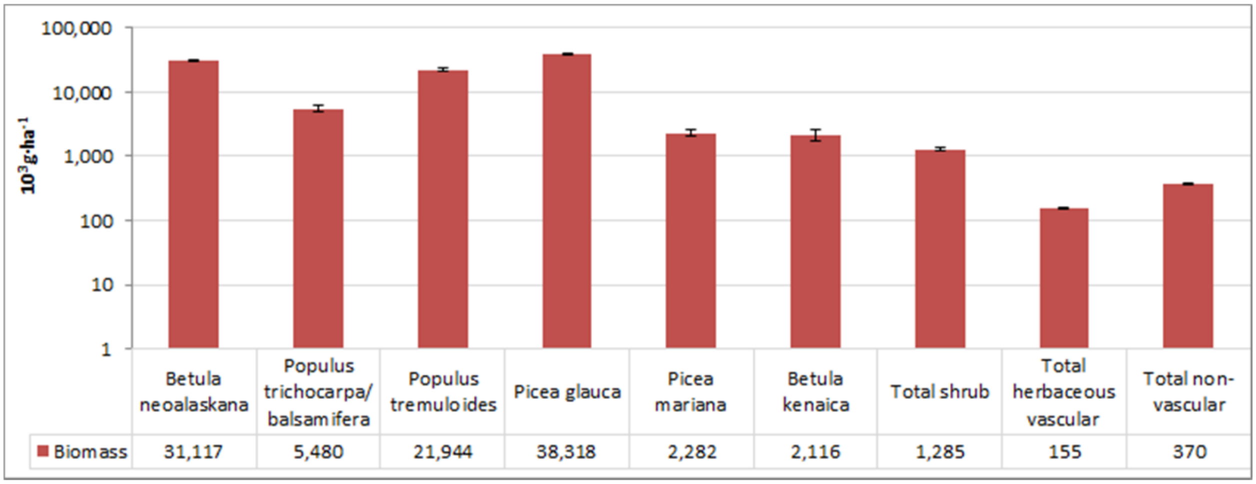

Fig. S3 Total above-ground biomass (AGB) by species and plant type with standard error bars.

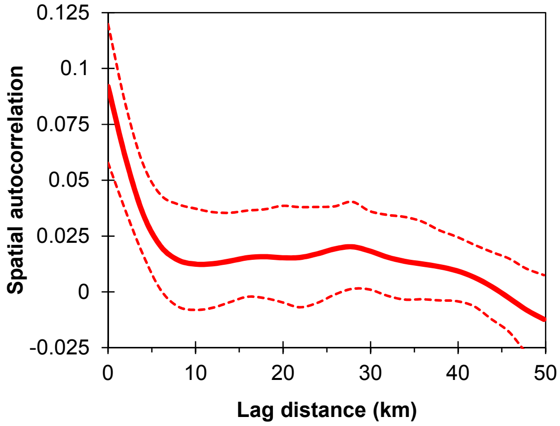

Fig. S4 Mean (solid line) and 95% confidence intervals (dashed lines) of the nonparametric spatial covariance function, showing local spatial autocorrelation in values of above-ground net primary productivity, and a range of spatial dependence of ~10 km.

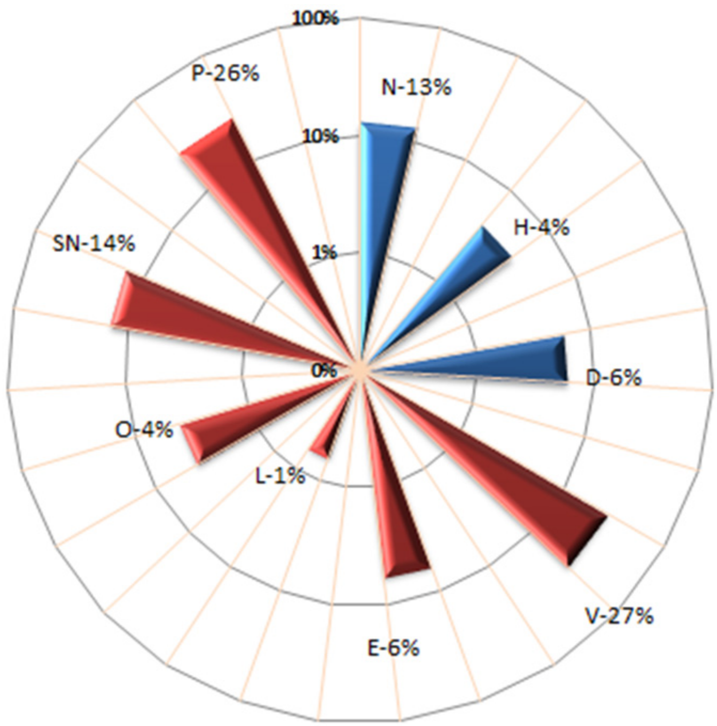

Fig. S5 Independent contribution of biodiversity measures (blue wedges) and control variables (red wedges) to the goodness-of-fit of individual ANPP.

Table S1 | List of plant species. A total of 283 coexisting plant species studied in this paper are categorized into nine general functional groups—tree, shrub, forb, grass and rush, sedge, fern, lichen, moss, and liverwort.

		Tree			
1	*Betula kenaica*	5	*Larix laricina*	9	*Populus trichocarpa*
2	*Betula neoalaskana*	6	*Picea mariana*	10	*Tsuga mertensiana*
3	*Betula papyrifera*	7	*Populus tremuloides*	11	*Picea lutz*
4	*Picea glauca*	8	*Populus balsamifera*		
		Shrub			
1	*Alnus tenuifolia*	19	*Ledum palustre*	37	*Salix arctica*
2	*Alnus viridis (crispa)*	20	*Linnaea borealis*	38	*Salix bebbiana*
3	*Amelanchier alnifolia*	21	*Menziesia ferruginea*	39	*Salix myrtillifolia*
4	*Andromeda polifolia*	22	*Oplopanax horridus*	40	*Salix phylicfolia*
5	*Arctostaphlos rubra*	23	*Oxycoccus microcarpus*	41	*Salix pulchra*
6	*Arctostaphlos uva-ursi*	24	*Potentilla fruticosa*	42	*Salix reticulata*
7	*Betula glandulosa*	25	*Potentilla palustris*	43	*Salix* species
8	*Betula nana*	26	*Rhododendron lapponicum*	44	*Sambucus racemosa*
9	*Cassiope tetragona*	27	*Ribes glandulosom*	45	*Shepherdia canadensis*
10	*Chamaedaphne calyculata*	28	*Ribes hudsonianum*	46	*Sorbus scopulina*
11	*Dryas integrifolia*	29	*Ribes lacustre*	47	*Spiraea Beauverdiana*
12	*Dryas octopetala*	30	*Ribes triste*	48	*Vaccinium caespitosum*
13	*Empetrum nigrum*	31	*Rosa acicularis*	49	*Vaccinium ovalifolium*
14	*Juniperus horizontalis*	32	*Rosa nutkana*	50	*Vaccinium oxycoccos*
15	*Juniperus scopulorum*	33	*Rubus arcticus*	51	*Vaccinium uliginosum*
16	*Juniperus communis*	34	*Rubus chamaemorus*	52	*Vaccinium vitis-idaea*
17	*Ledum glandulosum*	35	*Rubus idaeus*	53	*Viburnum edule*
18	*Ledum groenlandicum*	36	*Rubus pedatus*		
		Herbaceous Vascular—Forb			
1	*Achillea borealis*	41	*Equisetum arvense*	81	*Polygonum alaskanum*
2	*Aconitum delphinifolium*	42	*Equisetum pratense*	82	*Polemonium boreale*
3	*Actaea rubra*	43	*Equisetum scirpoides*	83	*Polemonium pulcherrimum*
4	*Allium schoenoprasum*	44	*Equisetum sylvaticum*	84	*Polygonum viviparum*
5	*Anemone canadensis*	45	*Fragaria virginiana*	85	*Primula incana*
6	*Anemone multifida*	46	*Galium boreale*	86	*Primula tschuktschorum*
7	*Anemone parviflora*	47	*Galium triforum*	87	*Pulsatilla patens*
8	*Anenome richardsonii*	48	*Gentiana propinqua*	88	*Pyrola asarifolia*
9	*Angelica lucida*	49	*Geocaulon lividum*	89	*Pyrola chlorantha*
10	*Antennaria pulcherrima*	50	*Geranium erianthum*	90	*Pyrola grandiflora*
11	*Arabis holboellii*	51	*Goodyera repens*	91	*Pyrola minor*
12	*Arnica alpina*	52	*Hedysarum alpinum*	92	*Ranunculus gmelini*
13	*Arnica Lessingii*	53	*Heracleum lanatum*	93	*Ranunculus lapponicus*
14	*Artemisia Tilesii*	54	*Hieracium triste*	94	*Ranunculus nivalis*
15	*Aster alpinus*	55	*Iris setosa*	95	*Ranunculus reptans*
16	*Astragalus americanus*	56	*Lathyrus palustris*	96	*Rumex arcticus*
17	*Aster junciformis*	57	*Listera cordata*	97	*Sanguisorba officinalis*
18	*Aster sibiricus*	58	*Lupinus arcticus*	98	*Sanguisorba stipulata*
19	*Astragalus umbellatus*	59	*Lycopodium alpinum*	99	*Saussurea angustifolia*
20	*Boschniakia rossica*	60	*Lycopodium annotinum*	100	*Senecio lugens*
21	*Boykinia richardsonii*	61	*Lycopodium clavatum*	101	*Senecio triangaris*
22	*Bupleurum triradiatum*	62	*Lycopodium complanatum*	102	*Senecio vulgaris*
23	*Calypso bulbosa*	63	*Mertensia paniculata*	103	*Smilacina stellata*
24	*Campanula lasiocarpa*	64	*Mimulus guttatus*	104	*Solidago decumbens*
25	*Campanula rotundifolia*	65	*Moehringia lateriflora*	105	*Solidago multiradiata*
26	*Castilleja caudata*	66	*Monesus uniflora*	106	*Spiranthes Romanzoffiana*
27	*Cassiope tetragona*	67	*Orthilia secunda*	107	*Stellaria crassifolia*
28	*Castilleja unalaschcensis*	68	*Osmorhiza depauperata*	108	*Stellaria longifolia*
29	*Chamerion angustifolium*	69	*Oxytropis campestris*	109	*Stellaria media*
30	*Circaea alpina*	70	*Parnassia palustris*	110	*Streptopus amplexifolius*
31	*Cnidium cnidiifolium*	71	*Pedicularis capitata*	111	*Taraxacum officinale*
32	*Corydalis aurea*	72	*Pedicularis labradorica*	112	*Thalictrum alpinum*
33	*Corydalis pauciflora*	73	*Pedicularis Langsdorffii*	113	*Thalictrum sparsiflorum*
34	*Cornus canadensis*	74	*Pedicularis verticillata*	114	*Trientalis europaea*
35	*Corallorrhiza trifida*	75	*Petasites frigidus*	115	*Valeriana capitata*
36	*Cypripedium passerinum*	76	*Petasites hyperboreus*	116	*Veratrum viride*
37	*Delphinium brachycentrum*	77	*Petasites sagittatus*	117	*Viola epipsila*
38	*Delphinium glaucum*	78	*Platanthera hyperborea*	118	*Viola palustris*
39	*Dodecatheon frigidum*	79	*Platanthera obtusata*	119	*Zygadenus elegans*

40	*Drosera rotundifolia*	80	*Polemonium acutiflorum*		
		Herbaceous Vascular—Grass and Rush			
1	*Calamagrostis canadensis*	5	*Parnassia palustris*	9	*Poa palustris*
2	*Elymus* species	6	*Poa arctica*	10	*Poa* species
3	*Festuca altaica*	7	*Poa glauca*	11	unknown grass
4	*Oryzopsis asperifolia*	8	*Poa juncifolia*	12	Juncaceae species
		Herbaceous Vascular—Sedge			
1	*Carex glacialis*	3	*Eriophorum angustifolium*	5	unknown sedge
2	*Carex* species	4	*Eriophorum* species		
		Herbaceous Vascular—Fern			
1	*Athyrium felix-femina*	3	*Dryopteris expansa*	5	*Woodsia glabella*
2	*Dryopteris dilatata*	4	*Gymnocarpium dryopteris*	6	unknown fern
		Non-Vascular—Lichen			
1	*Bryoria fuscessens*	18	*Cladonia deformis*	35	*Nephroma* species
2	*Cetraria cucullata*	19	*Cladonia ecmocyna*	36	*Pannaria pezizoides*
3	*Cetraria deliseii*	20	*Cladonia gracilis*	37	*Parmeliopsis ambigua*
4	*Cetraria islandica*	21	*Cladina mitis*	38	*Parmelia sulcata*
5	*Cetraria nivalis*	22	*Cladonia multiformis*	39	*Peltigera aphthosa*
6	*Cetraria pinastri*	23	*Cladina rangiferina*	40	*Peltigera canina*
7	*Certraia tilesii*	24	*Cladonia squamosa*	41	*Peltigera malacea*
8	*Cirriphllum cirrosum*	25	*Cladina stellarus*	42	*Peltigera neopolydactyla*
9	*Cladonia bellidiflora*	26	*Cladonia uncialis*	43	*Peltigera polydactyla*
10	*Cladonia botrytes*	27	*Dactylina arctica*	44	*Peltigera venosa*
11	*Cladonia cariosa*	28	*Evernia mesomorpha*	45	*Platismatia glauca*
12	*Cladonia cenotea*	29	*Hypogymnia physodes*	46	*Rhytidium rugosum*
13	*Cladonia chlorophaea*	30	*Lobaria linita*	47	*Stereocaulon alpinum*
14	*Cladonia coccifera*	31	*Lobaria pulmonaria*	48	*Stereocaulon* species
15	*Cladonia coniocraea*	32	*Masonhalea richardsonii*	49	*Usnia subfloridana*
16	*Cladonia cornuta*	33	*Nephroma arcticum*	50	unknown lichen
17	*Cladonia crispata*	34	*Nephroma expallidum*		
		Non-Vascular—Moss			
1	*Aulacomnium palustre*	9	*Hylocomium splendens*	17	*Ptilium crista-castrensis*
2	*Aulacommium turgidum*	10	*Hypnum subimponens*	18	*Rhizomnium glabrescens*
3	*Brachythecium salebrosum*	11	*Philontis fontana*	19	*Sphagnum* species
4	*Campylium stellatum*	12	*Plagiomnium medium*	20	*Splachnum luteum*
5	*Climacium dendroides*	13	*Pleurozium schreberi*	21	*Thuidium abietinum*
6	*Dicranum* species	14	*Polytrichum commune*	22	*Timmia ausstriaca*
7	*Drepanocladus uncinatus*	15	*Polytrichum juniperinum*	23	*Tomenthypnum nitens*
8	*Hedwigia ciliata*	16	*Polytrichum piliferum*	24	unknown moss
		Non-Vascular—Liverwort			
1	*Lepidozia reptans*	2	*Lophozia ventricosa*	3	*Marchantia polymorpha*

Table S2 | Definition, unit, and summary statistics of the variables used in this study.

Variable	Definition	Unit	Mean	Std.	Min.	Max.
Response variables						
$ANPP_{ijk}$	Aboveground net primary productivity of the *k*th tree of plot *j* and species *i* (individual-level ANPP)	$10^3 g \cdot ha^{-1} \cdot y^{-1}$	31.84	49.81	-1811.58	1583.14
Biodiversity measures						
N_j	Richness of all the plant species of plot *j*		18.93	4.90	1.00	39.00
H_j	Shannon index		0.56	0.32	0.00	1.31
D_j	Simpson index/HHI		0.30	0.20	0.00	0.69
Control variables						
V	Total AGB biomass at the previous inventory (5 years before current inventory)	$10^3 g \cdot ha^{-1}$	103014.48	48421.98	3330.30	343300.47
E	Plot elevation obtained from GPS unit	m	110.15	68.48	5.37	292.10
L	Percentage slope of a plot		11.50	14.37	0.00	77.00
O	Thickness of all surface organic horizons	cm	11.83	10.69	1.27	109.22
SN	Number of snags		18.72	19.79	0.00	119.00
P	Number of *Picea glauca* individuals in comparative relationship to the total number of trees on a plot		0.37	0.34	0.00	1.00
Temporal variables						
T_1	First time indicator that takes the value 1 if current inventory is the *third* inventory and 0 if otherwise		0.33	0.47	0.00	1.00
T_2	Second time indicator that takes the value 1 if current inventory is the *fourth* inventory and 0 if otherwise		0.08	0.28	0.00	1.00
Geographic coordinates						
λ	Easting of UTM coordinates	10^6m	0.52	0.10	0.34	0.66
φ	Northing of UTM coordinates	10^6m	6.94	0.17	6.66	7.24

Table S3 | Estimates and goodness-of-fit of the spatio-temporal model supporting N–E. Initial explanatory variables were selected with HP, and parameters were estimated using GLS. Biodiversity variables and their significance levels were in shade.

Shannon Index			Simpson Index/HHI		
Var	**Coef**	**95% C.I.**	***Var***	**Coef**	**95% C.I.**
const	12.34	(11.66, 13.02)	*const*	13.25	(12.63, 13.86)
H	10.51	(8.80, 12.22)	D	16.10	(13.11, 19.09)
H^2	-3.87	(-5.32, -2.42)	D^2	-8.27	(-13.06, -3.47)
V	0.00015	(0.00015, 0.00016)	V	0.00015	(0.00014, 0.00015)
SN	-0.20	(-0.21, -0.19)	SN	-0.20	(-0.21, -0.20)
P	15.19	(14.64, 15.73)	P	15.05	(14.51, 15.59)
T_1	-2.05	(-2.40, -1.71)	T_1	-2.06	(-2.41, -1.72)
T_2	-5.63	(-6.15, -5.10)	T_2	-5.69	(-6.21, -5.17)
AIC	4259.10		***AIC***	4260.24	
BIC	4358.65		***BIC***	4359.79	
n	470513		***n***	470513	

const: constant
AIC: Akaike information criterion
BIC: Bayesian information criterion
n: number of observations that is used in the bootstrap simulation